lubricants

IMPACT FACTOR 3.5

CITESCORE 4.1

Review

Influence of Parasitic Electric Currents on an Exemplary Mineral-Oil-Based Lubricant and the Raceway Surfaces of Thrust Bearings

Simon Graf, Oliver Koch and Bernd Sauer

Special Issue
Behavior of Lubricated Bearings in Electric Circuits
Edited by
Prof. Dr. Eckhard Kirchner and Dr. Marcel Bartz

MDPI

https://doi.org/10.3390/lubricants11080313

lubricants

MDPI

Review

Influence of Parasitic Electric Currents on an Exemplary Mineral-Oil-Based Lubricant and the Raceway Surfaces of Thrust Bearings

Simon Graf *, Oliver Koch and Bernd Sauer

Chair of Machine Elements, Gears and Tribology (MEGT) RPTU Kaiserslautern-Landau, Gottlieb Daimler Straße 42, 67663 Kaiserslautern, Germany
* Correspondence: s.graf@mv.uni-kl.de; Tel.: +49-0631-205-3716

Abstract: Within this paper, electro-mechanical long-term tests on a thrust bearing were presented. The effects of an additional electrical load on the bearing raceways and the used lubricant were investigated. Chemical investigations and viscosity measurements were presented, which show the changes in the lubricant. These investigations were compared with the electrical loads and the occurring raceway damage. In addition, a comparison was made with mechanical reference tests. This procedure makes it possible to classify the changes that occur due to the electrical load and to distinguish the effects from each other. The background to these investigations is the increased occurrence of parasitic currents in electric motors, which can lead to damage to machine elements. The phenomena that occur here are new challenges in the development of drive trains.

Keywords: bearing currents; electrical properties of lubricants; influence analysis

Citation: Graf, S.; Koch, O.; Sauer, B. Influence of Parasitic Electric Currents on an Exemplary Mineral-Oil-Based Lubricant and the Raceway Surfaces of Thrust Bearings. *Lubricants* **2023**, *11*, 313. https://doi.org/10.3390/lubricants11080313

Received: 30 June 2023
Revised: 19 July 2023
Accepted: 21 July 2023
Published: 25 July 2023

1. Introduction

Due to the increasing use of AC machines in combination with fast-switching frequency converters, there is an increased electrical load on machine elements (cf. summary according to [1,2]). In this case, the parasitic current flows mostly via the tribological contacts. As a result of the interaction between this additional electrical and the mechanical load on the contact, the components can be damaged and their service life reduced [3–5]. This affects not only the metallic raceway surfaces of bearings and gears, but the lubricant which separates the contact partners is also affected [6–8]. Therefore, the lubricant must also be considered as an electrical component.

The most important electrical parameters of the lubricants are as follows:

- The relative permittivity ε_r gives the electrical polarization ability of a dielectric;
- The breakdown field strength E (also breakdown voltage) indicates the highest field strength that can be applied to a material without it failing as an insulating medium;
- The specific electrical resistance ρ or its reciprocal, the electrical conductivity κ, describes the electrical conductivity of a material.

In addition, a rough distinction is made between high- and low-resistance lubricants [9,10].

In combination with the rheological lubricant properties (such as viscosity and density), these electrical variables influence the properties and effects of the bearing currents. Another component influencing the properties is any possible additive in the lubricant. Even with purely mechanical loads, individual additives or combinations of various additive packages can influence the service life of a lubricant both positively and negatively. In the context of the increasing electrification of powertrains, the demands on lubricants have increased even further [11]. The choice of lubricant can influence both the magnitude of the bearing voltage amplitude [5,6,9,12,13] and the damaging effects on the rolling bearing components [5,11,14–16]. Here, for example, investigations on single-contact test rigs show

increased wear under combined electro-mechanical load depending on the lubricant [15]. So-called "tribo-electro-chemical" reactions also occur [7]. These describe the interaction between the conditions in the tribological contact, the external electrical load, and the resulting changes in the lubricant chemistry. Both the processes of absorption/desorption of the additives in the electric field and the influence of the reactions of the lubricant with the contact surface by the passage of electric current should be mentioned [7]. These are shown, for example, by changes in the lubricant at the molecular level [17] (the changes observed here led to an increased occurrence of white etching cracks). Furthermore, the electrical and dielectric properties can also be influenced by the addition of additives [8].

In the context of investigations with electrically loaded lubricants, infrared spectroscopy (IR-spectroscopy) was successfully used for analysis by [10,18–20]. Here, however, partly contradictory results are shown depending on the author.

In the context of the investigations presented here, results from long-term tests are presented in which, in addition to the electro-mechanical damage to the rolling surfaces, the lubricant is also investigated.

2. Materials

A thrust-bearing test rig was used to investigate the issue specified here. This was developed as part of the research project [5] and allows the targeted investigation of the interaction between mechanical and electrical loads. This test adapter with the designation GESA (*ger. Gerät zur erweiterten Schmierstoffanalyse-device for advanced lubricant analysis*) can be operated in a four-ball apparatus. The reliability and quality of this test system have been demonstrated in a large number of publications [6,21–24]. A schematic sketch of the test fixture is shown in Figure 1.

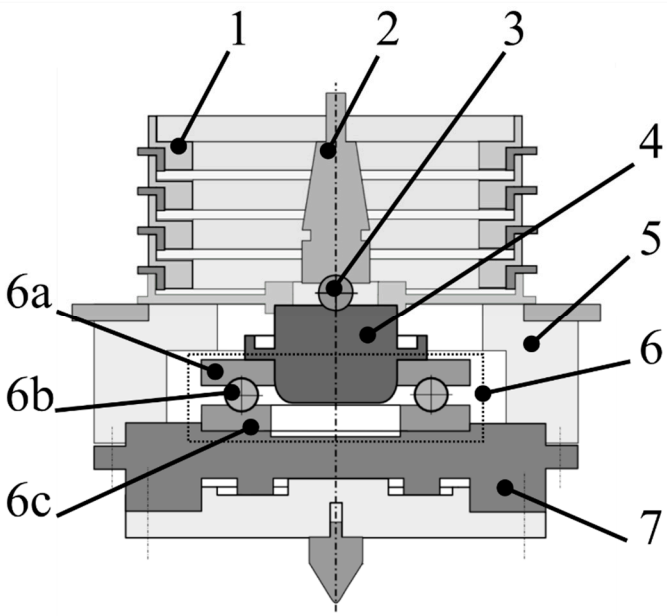

Figure 1. Sectional view of GESA (1 distributing ring/2 driving shaft/3 centering ball/4 shaft/5 housing/6 tested bearing/6a rotating ring/6b rolling element/6c stationary ring/7 bearing ring holder).

A thrust bearing of type 51208 (cf. Table 1) and a non-additive mineral oil with the designation OF 1.1 (cf. Table 2) serve as the test objects in this case.

The applied electrical load corresponds to a common-mode voltage whose frequency and voltage amplitude can be adjusted. A specially developed signal generator was used for this purpose. This allows the rolling bearing to be subjected to an electrical load comparable to that in the real electrical machine.

Table 1. Summary of the geometric dimensions as well as an indication of essential calculation data and surface characteristics of the test bearing 51208.

Geometrical Data			Surface and Calculation Data	
d:	42 mm	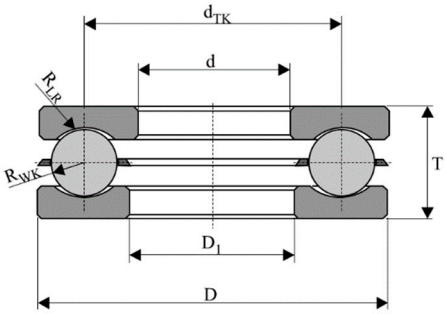	C:	35.2 kN
d_{TK}:	53 mm		C_0:	77.6 kN
D:	68 mm		n_{limit}:	4400 min^{-1}
D_1	40 mm		Sa *:	0.51 µm
R_{LR} *:	5.8 mm		Sq *	0.64 µm
R_{WK} *:	5.15 mm		Sk *	1.53 µm
T:	19 mm		Spk *	0.32 µm
			Svk *	0.89 µm

* Median of 26 single measurements by using a confocal microscope.

Table 2. Relevant properties of the used lubricant–mineral oil (OF 1.1).

Temperature/°C	10	40	80
Kinematic viscosity/mm^2/s	816.8	104.8	19.2
Density/g/cm^3	0.89	0.87	0.85
Conductivity/nS/m		<0.001	
Relative permittivity/-		2.15	

3. Experiment Description and Boundary Conditions

The following tests were carried out on the test set-up described above. A constant load was applied over the duration of the test and the long-term effects of these loads on the test specimen (thrust bearing 51208 and lubricating oil OF 1.1) were investigated. Figure 2 shows an example of the basic test procedure including the measured variables. In the beginning, the surfaces of the raceways of the axial bearings were examined and recorded with a microscope. In order to create comparable conditions for all tests, the actual test was preceded by a mechanical running-in phase that is identical for all test specimens. During this phase, the roughness peaks of the raceway surfaces were smoothed and a constant mechanical-electrical behavior was established [6,21–23]. As operating conditions, an operating time of 16 h, an axial load of 2400 N, and a speed of 1000 rpm were used. The lubricant used was further tempered to 40 °C and corresponded to the same type that is also used in the load phase. There was no electrical load within the run-in.

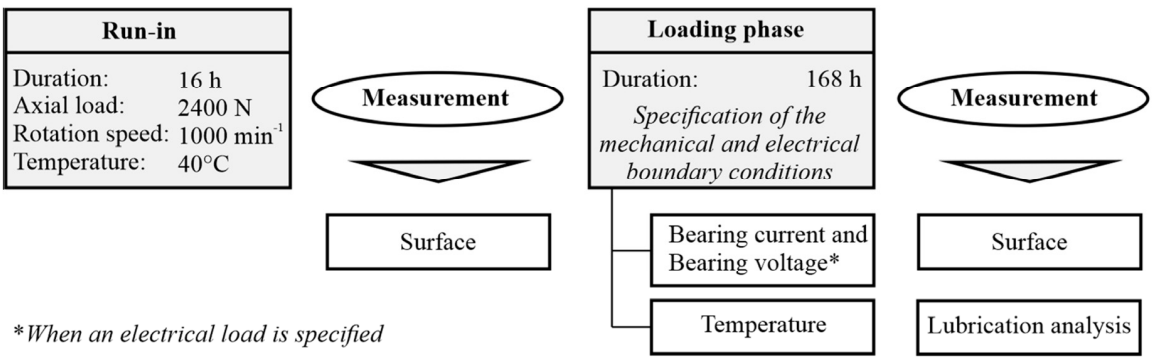

Figure 2. Schematic representation of the test sequence of the endurance tests with indication of the individual measured variables.

These preparatory steps are followed by the actual test run, which lasts 168 h. For this purpose, the test cell was cleaned beforehand and the run-in test specimen was supplied

with fresh lubricating oil. Furthermore, the boundary conditions of the individual test runs were applied. These boundary conditions are listed in Table 3 together with the designation of the individual tests. After completion of the loading phase, the test cell was dismantled and the loaded lubricant was filled for further oil analysis. In addition, the bearings were inspected and the surface changes are documented. During the running-in phase and the load phase, various measured variables were recorded. Furthermore, in the case of additional electrical load, the bearing currents and bearing voltages were recorded. By selecting the test parameters according to Table 3, the influence of various variables and their effects on the test specimen were determined with as few tests as possible. Furthermore, the results from endurance tests known from the literature should be taken into account when selecting the operating conditions.

Table 3. Boundary conditions specified at the test bench.

Designation	Force/N	Rotation Speed/rpm	Temperature/°C	Common-Mode-Voltage/V (pk to pk)	Switching Frequency/kHz
A-m1	4000	1000	40	-	-
A-m2			80		
A-e1	4000	1000	40	60	20
A-e2			40	40	
A-e3 *			40	20	
A-e4			80	60	
B-m1	6000	1000	40	-	-
B-e1	6000	1000	40	60	20
B-e2			40		5
B-e3			80		20
C-m1	8000	1000	40	-	-
C-e1	8000	1000	40	60	20

* including retry with -a and -b denoted.

To assess the mechanical load on a rolling bearing, rolling bearing manufacturers use the ratio between the static load capacity ($C0$) and the equivalent dynamic bearing load (P). So far, tests have mainly been carried out at low load ratios of the rolling bearings ($C0/P \leq 32$). Accordingly, the mechanical load points applied for this series of tests were selected so that higher load conditions occur in the rolling contact. For this purpose, the following three primary test series were defined:

- Test series A—axial load 4000 N ($C0/P$ 19);
- Test series B—axial load 6000 N ($C0/P$ 13);
- Test series C—axial load 8000 N ($C0/P$ 10).

The operating speed for each test was 1000 min^{-1} at partly different lubricant temperatures (40 °C and 80 °C). As a result of these mechanical operating conditions, the loads and lubricant film heights in the tribological contact listed in Table 4 occur based on the formal behavior conform to [24]. In order to be able to distinguish the electrical changes from normal, purely mechanical changes, mechanical reference tests are carried out in each test series. These serve as a basis for assessing and interpreting the combined mechanical and electrical loads. Based on this reference, each test series is loaded with the electrical peak-to-peak voltage of 60 V (corresponds approximately to the proportion of the DC link voltage of the electrical machine which is present at the rotor bearings as electrical potential) at 20 kHz switching frequency. This basic test should allow conclusions to be drawn about the interaction of mechanical load, lubricant film height, and the electrical load parameters in relation to the changes in the rolling bearing components and the lubricant.

Table 4. Mechanical parameters at the test bench.

Parameter	Unit	Test Series A	Test Series B	Test Series C
Contact force	N	4000	6000	8000
C0/P	-	19	13	10
Hertzian pressure	MPa	1494	1710	1883
Single contact area	mm^2	0.27	0.35	0.43
Lubrication gap height *	µm	0.79 @40 °C 0.22 @80 °C	0.76 @40 °C 0.21 @80 °C	0.72 @40 °C -
Specific lubrication gap	-	1.23 @40 °C 0.34 @80 °C	1.19 @40 °C 0.33 @80 °C	1.13 @40 °C -

* according to [25].

Test series A (4000 N/$C0/P$ 19) was then subjected to a voltage variation of 60 V, 40 V, and 20 V common mode voltage at the bearing. The aim here is to investigate the effects of the voltage amplitude on the surface change. Furthermore, the influence of the lubricant temperature is also investigated in this series of tests. Increasing the temperature led to a decrease in the breakdown voltage as well as a strong reduction of the lubricant film. Both effects led to a current transfer in the contact at a lower voltage amplitude. A mechanical reference test was also carried out at an increased temperature as part of this series of tests. To check the reproducibility of the tests, the test configuration A-e3 was repeated under the same conditions (A-e3-a/A-e3-b).

Test series B (6000 N/$C0/P$ 13) was also carried out with increased lubricant temperature, as in test series A (4000 N/$C0/P$ 19). This is to investigate the interaction due to the increase of the Hertzian contact area with the resulting decrease of the bearing current density (with identical source voltage applied to the bearing). Furthermore, an additional test with reduced clock frequency of 5 kHz was carried out and it was determined whether there was a correlation with the degree of the observed changes.

Test series C (8000 N/$C0/P$ 10) is intended to show the influence of further increased contact pressures. No further variation took place within this test series. Table 4 summarizes the mechanical parameters for interpreting the loads in the rolling contact for the individual test series.

4. Results

4.1. Electrical Load over Time

In order to ensure comparability with endurance tests known from the literature, the known design parameters are listed in Table 5 as an average over the entire test. In addition to the mean apparent bearing current density and the mean bearing apparent power, the electrical bearing stress W defined according to [18] is also given here. The electrical bearing stress is defined by the multiplication of the apparent bearing current density J_C, the switching frequency f_c of the frequency inverter, and the operating time $t_{operation}$ of the electrical load ($W = J_C \times f_c \times t_{operation}$). The average number of discharges is also listed in Table 5.

Table 5. Electrical loads determined over the test time.

Designation	Apparent Bearing Current Density/A/mm^2	Bearing Apparent Power/VA	Bearing Stress/10^9 A/mm^2	Average Discharge Frequency/Hz
A-e1	0.16	4.13	19.35	17,860
A-e2	0.10	2.04	12.10	16,978
A-e3-a	0.05	0.78	0.60	14,647
A-e3-b	0.05	0.70	0.60	16,692
A-e4	0.15	3.97	18.14	15,398

Table 5. *Cont.*

Designation	Apparent Bearing Current Density/A/mm^2	Bearing Apparent Power/VA	Bearing Stress/10^9 A/mm^2	Average Discharge Frequency/Hz
B-e1	0.11	4.02	13.31	18,301
B-e2	0.11	3.67	13.31	4690
B-e3	0.12	4.01	14.52	17,990
C-e1	0.08	3.93	0.97	10,788

Furthermore, the electrical stresses for the individual tests are visualized in Figure 3 by means of the boxplots known from statistics. Here, the standard deviation is not shown due to the exponential distribution of the data and, instead, the 25% and 75% quantiles were used. The reason for this is that these statistical parameters better indicate a rightward or leftward skew in the data distribution. This representation allows a compromise between the singular characteristic value from Table 5 and a detailed oscillographic representation at several test times.

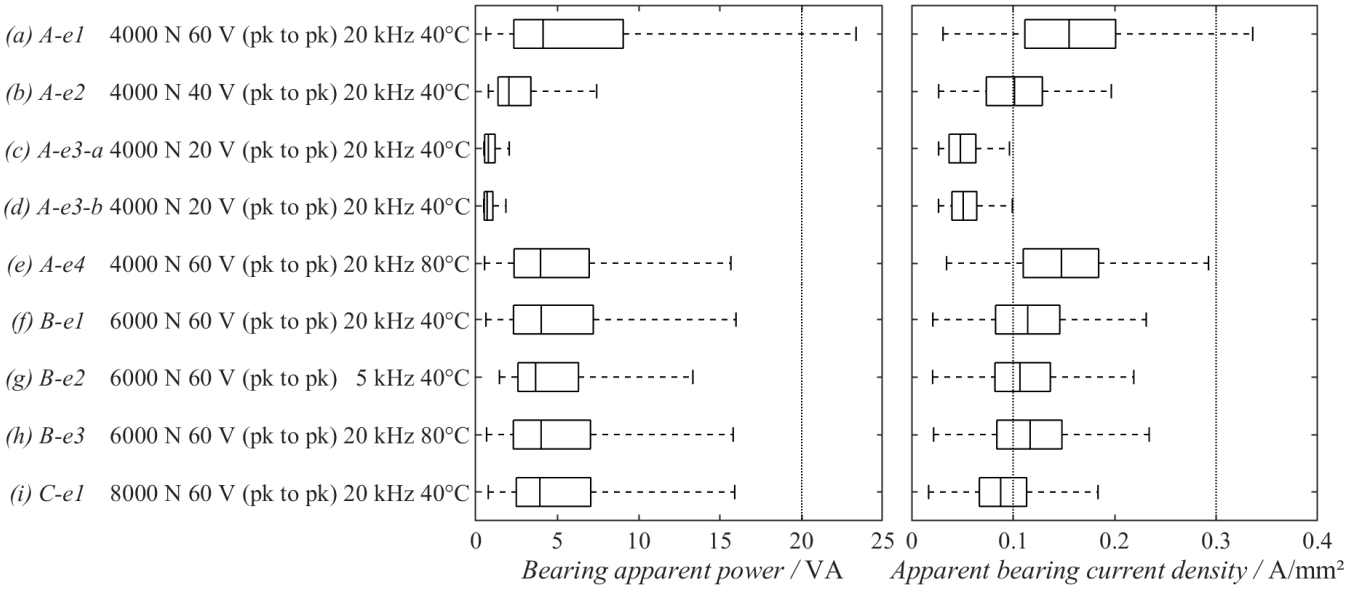

Figure 3. Representation of the boxplots of the individual tests for bearing apparent power and bearing current density with minimum value, 25% quantile, mean value, 75% quantile, and maximum value.

It is evident from the electrical loads that occur that they are predominantly within the permitted limits for the electrical bearing power and the apparent bearing current density.

4.2. Occurring Surface Changes

The surface changes that occur in the bearing raceways and the rolling elements are a result of the acting mechanical and electrical loads. The interaction between the tribological condition of the contact and the resulting electrical substitute system must be taken into account. Thus, a change in the tribological behavior of the rolling contact can occur due to the electrically induced surface mutation, which in turn influences the type of bearing current. Furthermore, the degree of damage to the bearing is classified by the type of surface change that occurs. Investigations into how the surface changes that occur during gray frosting affect the further service life of a rolling bearing are the subject of current research, such as [25].

Compared to long-term tests known from the literature, this work focused exclusively on tests with a high mechanical load ($C0/P < 20$). Regardless of the high load, every possible surface change that could occur in the context of an electromechanical load was also detected in these tests. Figure 4 shows exemplary macroscopic and microscopic images of the bearing raceways and rolling elements that occurred after the tests. In order to establish a reference to the influence of the electrical load, a picture of a purely mechanically loaded bearing is also shown (cf. Figure 4a Rolling bearing raceway and rolling elements). In addition to the clear surface conditions such as grey frosting (cf. Figure 4a EDM or ohmic based) and fluting (cf. Figure 4c), very fine periodically changing surface changes could also be detected (cf. Figure 4d). These are strongly reminiscent of the familiar flutings in their type and characteristics, but are much less pronounced and occur in the form of shading of raceways and rolling elements. This surface change will be referred to as fluting shading in the further course of the work. Whether this is a possible preliminary stage of fluting was not the focus of the tests carried out. Furthermore, circular ring-shaped structures appeared on individual rolling elements (cf. Figure 4e) as well as on the raceways (cf. Figure 4f). These are characterised by an undamaged surface surrounded by a circle of densely grouped craters. The shape and structure of these surrounding craters resembled those known from EDM currents. When this phenomenon occurred, only individual sections of the raceways or individual rolling elements were affected, but here there was an increased occurrence of these structures. These circular rings of craters are referred to in the following as bearing current marks. Based on the surface changes that occur, as shown in Figure 4, the different final states of the bearing surfaces are described below. Table 6, for example, shows which surface mutation has occurred on the individual components of the contact partners of the test bearings at the end of the respective tests.

Table 6. Visual assessment of the resulting surfaces after completion of the long-term tests.

Designation	Rotating Ring	Stationary Ring	Rolling Elements
A-m1	Mechanical run-in	Mechanical run-in	Mechanical run-in
A-m2	Mechanical run-in	Mechanical run-in	Mechanical run-in
A-e1	Fluting	Fluting shading	Bearing current marks
A-e2	Gray frosting	Gray frosting	Gray frosting
A-e3-a	No electrically induced change	Gray frosting	No electrically induced change
A-e3-b	No electrically induced change	Gray frosting	Gray frosting
A-e4	Gray frosting	Gray frosting	Gray frosting
B-m1	Mechanical run-in	Mechanical run-in	Mechanical run-in
B-e1	Gray frosting/Bearing current marks	Fluting shading	Bearing current marks
B-e2	Gray frosting/Bearing current marks	Gray frosting	Bearing current marks
B-e3	Gray frosting	Gray frosting	No electrically induced change
C-m1	Pitting	Pitting	Pitting
C-e1	Gray frosting	Pitting/ Gray frosting	Pitting/ Gray frosting

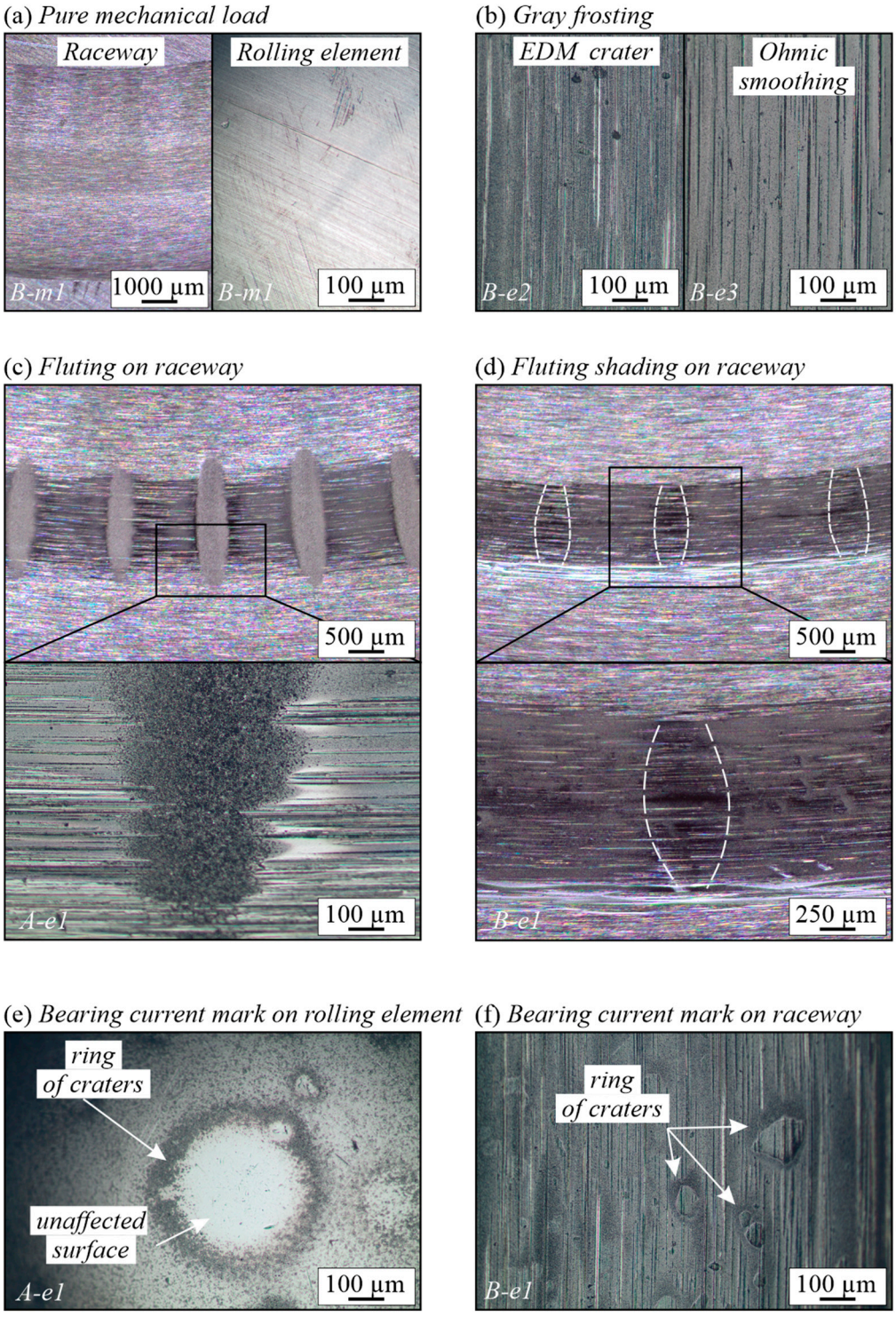

Figure 4. Surface changes that occurred during the endurance tests.

4.3. IR Spectroscopy

The examination of the contaminated oils showed an IR index greater than 99% for all tests. This means that each individual transmission diagram deviates at most 1% from the reference sample. For clarification, the individual measured spectra are summarized in Figure 5. In addition to the fresh oil curve, the total minima, maxima and mean values over all tests are shown. Within the IR bands between 750 cm^{-1} and 1100 cm^{-1}, there was a slight deviation in the minimum values from all experiments. This can be attributed to

test C-e1. The reason for this deviation seems to be the very strong wear including metallic chipping (cf. Table 6). Independent of this one exception, the results showed that there was no significant influence of the lubricant within the scope of this test series, which could be detected by IR spectroscopy. In [18,19], contrary results are published. In [18], a degradation of carboxylic acids (COOH group) could be determined in the grease used. This correlated to the level of bearing stress and thus to the electrical load.

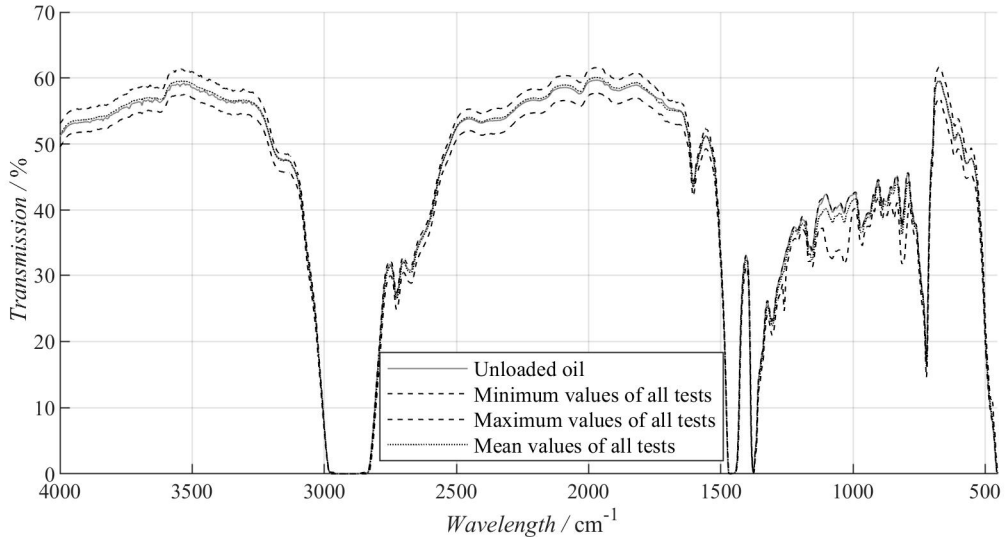

Figure 5. Comparison of the IR spectroscopies of the unloaded reference sample with the minimum, maximum, and mean values of all loaded oil samples.

In contrast, there are experimental results from [10,20] which correspond to the results presented here. In the spectroscopies carried out there, no deviation of the spectra between fresh and electrically loaded oil and consequently no correlation between current passage and lubricant ageing could be determined. Surface changes were also observed in both studies, which are comparable to those presented in Figure 4. Accordingly, the IR in the present case is inconspicuous and inconclusive with regard to an assessment of the electrical aging of lubricants.

4.4. Chemical Wear Elements (cf. Table 7) and Contaminants (cf. Table 8)

The detailed analysis for contamination identifies the impurities visible to the naked eye in test series C as iron particles from bearing raceways and rolling elements. This is due to the chipping and pitting visible in the macroscopic observation of the bearing rings in this test series. In the other tests, the iron value as a wear indicator is in the low two-digit range. In individual tests (A-m1, A-e3-b and C-e1), an increased silicon concentration can be observed. The most probable cause for this is the contamination of the lubricant by abrasion of the slip ring carrier. A connection between the degree of electrical load and the concentration of wear particles cannot be clearly proven within the framework of this series of tests.

Table 7. Chemical wear elements in the lubricant after a loading phase of 168 h.

	Chemical Wear Elements in mg/kg								
Designation	**FE**	**Cr**	**Sn**	**Al**	**Ni**	**Cu**	**Pb**	**Mo**	**Mn**
Reference	-	-	-	-	-	-	-	-	-
A-m1	10								
A-m2	35	1						1	

Table 7. *Cont.*

	Chemical Wear Elements in mg/kg								
Designation	**FE**	**Cr**	**Sn**	**Al**	**Ni**	**Cu**	**Pb**	**Mo**	**Mn**
A-e1	17								
A-e2	16	1							
A-e3-a	6								
A-e3-b	14						1	1	
A-e4	98		1						
B-m1	10								
B-e1	9								
B-e2	23								
B-e3	14								
C-m1	40	1		1	1			1	
C-e1	44					8			

Table 8. Chemical impurities and additives in the lubricant after a loading phase of 168 h.

	Impurities				Additives in mg/kg					
Designation	**Si**	**K**	**Na**	**Li**	**Ca**	**Mg**	**Zn**	**P**	**Ba**	**S**
Reference	-	-	-	-	2	-	-	1	-	4036
A-m1	286	2	1	-	-	-	1	3	-	4056
A-m2	11	-	-	-	5	-	1	-	-	3684
A-e1	39	-	1	1	3	-	1	2	-	3869
A-e2	11	-	-	-	1	-	1	2	-	3933
A-e3-a	12	-	-	1	-	-	-	2	-	3810
A-e3-b	148	-	-	-	2	-	1	-	-	3915
A-e4	32	-	-	-	2	-	2	-	-	3831
B-m1	8	-	-	-	4	-	-	-	-	3640
B-e1	-	-	-	-	-	-	-	-	-	3721
B-e2	3	-	-	-	2	1	1	5	-	3829
B-e3	59	-	-	-	1	-	3	-	-	3901
C-m1	56	1	-	-	4	1	-	3	-	3807
C-e1	1007	-	-	-	2	-	1	4	-	3980

4.5. Viscosity (cf. Table 9)

The measured viscosity of all tests fluctuated slightly ($\leq$3%) around the value of the reference sample of 105 mm^2/s. However, there was an exception. Test A-e2 showed a significantly lower viscosity (40 °C) of 92.2 mm^2/s. This deviation of about 13% is considered an outlier, especially considering the second viscosity measurement at 80 °C, which with 10.78 mm^2/s is within the scatter of the tests. Based on this, it can be assumed that there was no influence on the viscosity in the present tests.

Table 9. Overview of the lubricant properties after a loading phase of 168 h with comparison to an unloaded reference sample.

Designation	**Viscosity at 40 °C /mm/s^2**	**Viscosity at 80 °C /mm/s^2**	**Oxidation index /-**	**Color Code /-**
Reference	105	10.8	-	1
A-m1	104.9	11.11	10	2.5
A-m2	104.9	10.91	25	5.5

Table 9. *Cont.*

Designation	Viscosity at 40 °C /mm/s^2	Viscosity at 80 °C /mm/s^2	Oxidation index /-	Color Code /-
A-e1	105.1	10.88	<5	2
A-e2	92.2	10.78	-	2
A-e3-a	104.5	10.78	7	1.5
A-e3-b	105.6	10.89	12	2
A-e4	105.3	10.79	30	6
B-m1	105.6	10.88	14	2.5
B-e1	105.4	10.88	10	2
B-e2	105.3	10.85	6	2
B-e3	105.8	10.91	35	4
C-m1	103.6	10.79	12	3
C-e1	105.4	10.74	10	3

5. Conclusions

On the basis of the investigations carried out here on the electrical load and the interaction with the changes occurring on the components in the current flow, the following partial statements and assessments of the evaluations made can be made:

- **Electrical load over the test period: significant**

During the evaluation of the tests, different methods of visualizing and documenting the electrical load over time were recorded. In terms of their level of detail, these range from a single characteristic value for the entire test to a time-resolved frequency distribution of electrical events per test. Furthermore, the known dimensioning parameters such as bearing current density, bearing apparent power, and bearing stress were also determined here. A comparison of these characteristic values with the stress limits known from the literature showed that the loads only exceeded the lower design characteristic values (bearing current density, bearing apparent power, bearing stress) for individual rare events. Despite this low load, critical surface damage, such as corrugations, occurred in the tests. Ref. [26] provided a possible explanation for this. It was observed here that when transferring the dimensioning parameters determined for a specific radial deep groove ball bearing to other bearing sizes, there are inconsistencies in the limit loads. Due to the use of the axial bearing, it is therefore unclear whether the limiting loads determined on a radial deep groove ball bearing also apply to this bearing type. The identical problem is also evident when using the bearing apparent power as a design variable.

As a compromise between a one-dimensional characteristic value and a more detailed frequency evaluation, a boxplot representation similar to [27] was established, which allows the evaluation of the test.

- **Change in the rolling surface: significant**

Changes occurred in the surface topographies of both the raceways and the rolling elements as a result of the electrical loads. These differed significantly from the topographies of the purely mechanical reference tests. The subjective evaluation of the surfaces by means of a light microscope (cf. Figure 4) showed that with increasing electrical load, the running track takes on an increasingly silvery sheen in which the machining grooves and running-in marks, as in the surrounding area, are no longer visible. This phenomenon is called grey frosting. In the majority of the present tests, the grey frosting was accompanied by a strong smoothing of the surfaces, the cause of which is assumed to be an ohmic current flow. Furthermore, these tests also showed that the smoothing is more pronounced on the stationary ring than on the rotating ring (cf. Table 6). In a stub test (B-e2) with the reduced switching frequency, a gray running track was also observed, but this stood out from the rest of the track due to a clustering of individual discharge craters. Likewise, fluting appeared on the raceway in test A-e1. Accordingly, even at low C0/P ratios, all known surface

changes associated with parasitic bearing currents could be observed [28–30]. In addition, so-called bearing current marks occurred in isolated cases (cf. Figure 4e,f). Furthermore, fluting shading was also observed. White etching cracks as in [17,31,32] could not be observed.

- **Lubricant analysis: further research necessary**

The analytical methods used showed no clear influence of an electrical load on the lubricant used. The IR spectroscopy as well as the rheological properties were approximately at the level of a fresh oil sample and were comparable to the mechanical reference tests. In the tests with chipping on the bearing, increased values of iron abrasion were observed. Furthermore, an increased concentration of silicon was present in selected tests. The reason for this is most likely an increased abrasion of the slip ring. Accordingly, an interaction between the electrical load and damage to the lubricant could not be determined with the analyses carried out, despite clear electrical surface damage. Even though the lubricant analysis was not the focus of the present work, it is evident that IR spectroscopy shows ambiguous results in the context of an electrical load (cf. [10,18–20]) and a correlation of different wear particles to the electrical load could not be established in the context of these tests. Whether further analyses (such as Remaining Useful Live Evaluation Routine (RULER) test (cf. [33,34]), Nuclear Magnetic Resonance (NMR) spectroscopy (cf. [35,36], or dielectric spectroscopy) can detect the influence of the electrical load and which interactions occur between individual additives and the electrical fields resulting from the electrical load is not shown by the series of tests presented here.

Author Contributions: Conceptualization, S.G. and O.K.; methodology, S.G.; investigation, S.G.; writing—original draft preparation, S.G.; writing—review and editing, O.K. and B.S.; All authors have read and agreed to the published version of the manuscript.

Funding: This work was carried out within the framework of the projects "Model for determining the thermal stress of lubricants as a result of mechanical and electrical loads in rolling contact" (Project No. SA898/25-1/407468812) and "Determination of ball bearing impedances under steady-state operating conditions by means of a further developed rolling contact model at full film lubrication" (Project No. SA898/32-1/470273159). Both are financially supported by the Deutsche Forschungsgemeinschaft (DFG) e.V. (German Research Foundation).

Conflicts of Interest: The authors declare no conflict of interest.

References

1. Schneider, V.; Behrendt, C.; Höltje, P.; Cornel, D.; Becker-Dombrowsky, F.M.; Puchtler, S.; Gutiérrez Guzmán, F.; Ponick, B.; Jacobs, G.; Kirchner, E. Electrical Bearing Damage, A Problem in the Nano- and Macro-Range. *Lubricants* **2022**, *10*, 194. [CrossRef]
2. Graf, S.; Capan, R.; Koch, O.; Sauer, B. Electrically induced damage of rolling bearings due to parasitic converter currents in electrical drive trains. In Proceedings of the International Commercial Vehicle Symposium, Kaiserslautern, Germany, 13–15 September 2022; ISBN 978-3-658-40782-7. [CrossRef]
3. Zika, T. Electric Discharge Damaging in Lubricated Rolling Contacts. Ph.D. Dissertation, Technische Universität Wien, Wien, Austria, 2010.
4. Kriese, M.; Wittek, E.; Gattermann, S.; Tischmacher, H.; Poll, G.; Ponick, B. Influence of bearing currents on the bearing lifetime for converter driven machines. In Proceedings of the 2012 International Conference on Electrical Machines, Marseille, France, 2–5 September 2012; pp. 1735–1739. [CrossRef]
5. Bechev, D. Prüfmethodik zur Charakterisierung der Elektrischen Eigenschaften von Wälzlagerschmierstoffen. Ph.D. Thesis, Technische Universität Kaiserslautern, Kaiserslautern, Germany, 2020.
6. Gonda, A.; Capan, R.; Bechev, D.; Sauer, B. The Influence of Lubricant Conductivity on Bearing Currents in the Case of Rolling Bearing Greases. *Lubricants* **2019**, *7*, 108. [CrossRef]
7. Spikes, H.A. Triboelectrochemistry: Influence of Applied Electrical Potentials on Friction and Wear of Lubricated Contacts. *Tribol. Lett.* **2020**, *68*, 90. [CrossRef]
8. García Tuero, A.; Rivera, N.; Rodríguez, E.; Fernández-González, A.; Viesca, J.L.; Battez, A.H. Influence of Additives Concentration on the Electrical Properties and the Tribological Behaviour of Three Automatic Transmission Fluids. *Lubricants* **2022**, *10*, 276. [CrossRef]
9. Weicker, M. Gleichtakteffekte bei Umrichtergespeisten Elektromotoren. Ph.D. Thesis, Technische Universität Darmstadt, Darmstadt, Germany, 2021.

10. Phrashad, H. *Tribology in Electrical Environments*; Elsevier: Amsterdam, The Netherlands, 2006.
11. Chen, Y.; Jha, S.; Raut, A.; Zhang, W.; Liang, H. Performance Characteristics of Lubricants in Electric and Hybrid Vehicles: A Review of Current and Future Needs. *Front. Mech. Eng.* **2020**, *6*, 571464. [CrossRef]
12. Tischmacher, H.; Gattermann, S. Einflussgrößen auf Lagerströme bei umrichtergespeisten Elektromotoren. *VDI-Berichte* **2022**, *2013*, 45–59.
13. Durkin, W.; Fish, G.; Dura, R. *Compositional Effects on the Electrical Properties of Greases*; elgi Eurogrease Q2: Hamburg, Germany, 2022.
14. Esmaeili, K.; Wang, L.; Harvey, T.J.; White, N.M.; Holweger, W. Electrical Discharges in Oil-Lubricated Rolling Contacts and Their Detection Using Electrostatic Sensing Technique. *Sensors* **2022**, *22*, 392. [CrossRef] [PubMed]
15. Erdemir, A.; Farfan-Cabrera, L.; Anderson, W.B. Comparative Tri Comparative Tribological Properties of Commercial Drivetrain Lubricants under Electrified Sliding Contact Conditions. In Proceedings of the 2nd STLE Tribology & Lubrication for E-Mobility Conference, Online, 30 November 2022.
16. Radnai, B. Wirkmechanismen bei Spannungsbeaufschlagten Wälzlagern. Ph.D. Thesis, Technische Universität Kaiserslautern, Kaiserslautern, Germany, 2016.
17. Holweger, W.; Bobbio, L.; Mo, Z.; Fliege, J.; Goerlach, B.; Simon, B. A Validated Computational Study of Lubricants under White Etching Crack Conditions Exposed to Electrical Fields. *Lubricants* **2023**, *11*, 45. [CrossRef]
18. Muetze, A. Bearing Currents in Inverter-Fed AC Motors. Ph.D. Thesis, TU Darmstadt D 17, Shaker Verlag, Aachen, 2004.
19. Recker, C.; Weicker, M. Einfluss der elektrischen Schmierfettleitfähigkeit auf Die Ausbildung von Lagerströmen bei umrichterbetriebenen 1.5 kW-Asynchronmotoren, Aachen, 2022. 5. VDI-Fachkonferenz—Schadensmechanismen an Lagern. Available online: https://www.vdi-wissensforum.de/weiterbildung-maschinenbau/schadensmechanismen-an-lagern/ (accessed on 31 July 2022).
20. Jagenbrein, A. Investigations of Bearing Failures due to Electric Current Passage. Ph.D. Thesis, Technische Universität Wien, Vienna, Austria, 2005.
21. Bechev, D.; Kiekbusch, T.; Sauer, B. *Characterization of Electrical Lubricant Properties for Modelling of Electrical Drive Systems with Rolling Bearings*; Forschungsvereinigung Antriebstechnik eV (FVA): Frankfurt, Germany, 2018; Volume 3.
22. Graf, S.; Werner, M.; Koch, O.; Götz, S.; Sauer, B. Breakdown voltages in thrust bearings: Behavior and Measurement. *Tribol. Trans.* **2023**, *66*, 488–496. [CrossRef]
23. Graf, S. Charakterisierung und Auswirkungen von Parasitären Lagerströmen in Mischreibung. Ph.D. Thesis, RPTU Kaiserslautern-Landau, Kaiserslautern, Germany, 2023.
24. Hamrock, J.B.; Dowson, D. Isothermal elastohydrodynamic lubrication of point contacts III: Fully Flooded Results. *J. Lubr. Technol.* **1977**, *99*, 264–275. [CrossRef]
25. Schneider, V.; Stockbrügger, J.O. *FVA 863 I—Stromdurchgang am Wälzlager*; FVA-Heft Nr. 1501: Frankfurt, Germany, 2022.
26. Gemeinder, Y. Lagerimpedanz und Lagerschädigung bei Umrichtergespeisten Antrieben. Ph.D. Thesis, Technische Universität Darmstadt, Darmstadt, Germany, 2016.
27. Joshi, A. Electrical Characterisations of Bearings. Ph.D. Thesis, Chalmers University of Technology, Gothenburg, Switzerland, 2019.
28. Kohaut, A. *Riffelbildung in Wälzlagern Infolge Elektrischer Korrosion*; Zeitschrift für angewandte Physik 1.5; FAG Kugelfischer G. Schäfer: Schweinfurt, Germany, 1948; pp. 197–211.
29. Zika, T.; Gebeshuber, I.C.; Buschbeck, F.; Preisinger, G.; Gröschl, M. Surface analysis on rolling bearings after exposure to defined electric stress. *Proc. Inst. Mech. Eng. Part J J. Eng. Tribolog* **2009**, *223*, 787–797. [CrossRef]
30. Didenko, T.; Pridemore, W.D. Electrical Fluting Failure of a Tri-Lobe Roller Bearing. *J. Fail. Anal. Preven.* **2012**, *12*, 575–580. [CrossRef]
31. Loos, J.; Bergmann, I.; Goss, M. Influence of high electrical currents on WEC formation in rolling bearings. *Tribol. Trans.* **2021**, *64*, 708–720. [CrossRef]
32. Pohrer, B.; Zuercher, M.; Tremmel, S.; Wartzack, S.; Schlücker, E. Einfluss des tribochemischen Schichtaufbaus auf die Ausbildung elektrisch induzierter Wälzlagerschäden. *Tribol. Und Schmier. Bd.* **2016**, *63*, 32–39.
33. Perez, J. Oxidative properties of lubricants using thermal analysis. *Thermochim. Acta* **2000**, 47–56. [CrossRef]
34. Maguire, E. Monitoring of Lubricant Degradation with RULER and MPC. Available online: http://urn.kb.se/resolve?urn=urn:nbn:se:liu:diva-57846 (accessed on 31 July 2022).
35. Rudszuck, T.; Förster, E.; Nirschl, H.; Guthausen, G. Low-field NMR for quality control on oils. *Magn. Reson. Chem.* **2019**, *57*, 777–793. [CrossRef]
36. Rudszuck, T.; Zick, K.; Groß, D.; Nirschl, H.; Guthausen, G. Dedicated NMR sensor to analyze relaxation and diffusion in liquids and its application to characterize lubricants. *Magn. Reson. Chem.* **2021**, *59*, 825–834. [CrossRef]